the plant journal

SEB Society for Experimental Biology

The Plant Journal (2016) **87,** 484–494 doi: 10.1111/tpj.13213

Serine and threonine residues of plant STN7 kinase are differentially phosphorylated upon changing light conditions and specifically influence the activity and stability of the kinase

Andrea Trotta[1,†], Marjaana Suorsa[1,†], Marjaana Rantala[1], Björn Lundin[2] and Eva-Mari Aro[1,*]

[1]*Molecular Plant Biology, Department of Biochemistry, University of Turku, Turku FI-20520, Finland, and*

[2]*Department of Biological and Environmental Sciences, University of Gothenburg, Gothenburg 405 30, Sweden*

Received 26 February 2016; revised 4 May 2016; accepted 9 May 2016; published online 2 August 2016.

*For correspondence (e-mail evaaro@utu.fi).

†These authors make an equal contribution to this work.

SUMMARY

STN7 kinase catalyzes the phosphorylation of the globally most common membrane proteins, the light-harvesting complex II (LHCII) in plant chloroplasts. STN7 itself possesses one serine (Ser) and two threonine (Thr) phosphosites. We show that phosphorylation of the Thr residues protects STN7 against degradation in darkness, low light and red light, whereas increasing light intensity and far red illumination decrease phosphorylation and induce STN7 degradation. Ser phosphorylation, in turn, occurs under red and low intensity white light, coinciding with the client protein (LHCII) phosphorylation. Through analysis of the counteracting LHCII phosphatase mutant *tap38*/*pph1*, we show that Ser phosphorylation and activation of the STN7 kinase for subsequent LHCII phosphorylation are heavily affected by pre-illumination conditions. Transitions between the three activity states of the STN7 kinase (deactivated in darkness and far red light, activated in low and red light, inhibited in high light) are shown to modulate the phosphorylation of the STN7 Ser and Thr residues independently of each other. Such dynamic regulation of STN7 kinase phosphorylation is crucial for plant growth and environmental acclimation.

Keywords: *Arabidopsis thaliana*, light-harvesting complex, STN7, phosphoproteomics, selected reaction monitoring.

INTRODUCTION

A number of chloroplast proteins undergoes various kinds of post-translational modifications (PTM), which regulate their activity, stability and interaction with other proteins (for a recent review, see (Lehtimaki *et al.*, 2015). Among them, reversible phosphorylation of several thylakoid proteins bears a well characterized role in regulation and optimization of photosynthetic reactions (Reiland *et al.*, 2009; Schonberg and Baginsky, 2012). For instance, phosphorylation of the light-harvesting complex (LHC) II proteins is crucial for balanced excitation energy distribution in the thylakoid membrane, as phosphorylation of the major LHCII proteins Lhcb1 and Lhcb2 is essential for optimal functional interactions between LHCII, Photosystem (PS) I and PSII (Pesaresi *et al.*, 2009; Grieco *et al.*, 2015; Liu *et al.*, 2015; Longoni *et al.*, 2015).

Elucidation of the function of the thylakoid membrane protein phosphorylation became possible after identification and characterization of the kinases and phosphatases responsible for their reversible phosphorylation. The serine/threonine-protein kinase7 (Stt7) phosphorylating the LHCII proteins was first identified from a green algae *Chlamydomonas reinhardtii* (hereafter: Chlamydomonas) (Depege *et al.*, 2003), and a few years later, its homologue STN7 was characterized from *Arabidopsis thaliana* (Arabidopsis) (Bellafiore *et al.*, 2005). A phosphatase protein THYLAKOID-ASSOCIATED PHOSPHATASE OF 38 KDA/PROTEIN PHOSPHATASE 1 (TAP38/PPH1, hereafter: TAP38), in turn, has been shown to dephosphorylate LHCII (Pribil *et al.*, 2010; Shapiguzov *et al.*, 2010). LHCII phosphorylation has been shown to reach its highest level at light intensities lower than those prevailing during the growth (Rintamaki *et al.*, 1997), and it occurs upon activation of STN7 via binding of plastoquinol to the cytochrome b_6f (Cyt b_6f) complex (Vener

et al., 1997). In contrast, exposure of plants to high light (HL) intensities leads to LHCII dephosphorylation (Rintamaki *et al.*, 2000) that has been shown to be accompanied by reduced thioredoxins (Rintamaki *et al.*, 2000; Martinsuo *et al.*, 2003), although the exact molecular mechanism has remained obscure. Importantly, the complete LHCII dephosphorylation in HL is only transient since acclimation even to bright sunlight re-establishes chloroplast redox balance and allows LHCII to reach again a moderately high phosphorylation level (Wientjes *et al.*, 2013). Thus the buffering system, provided by reversible LHCII phosphorylation, is kept functional upon acclimation of plants to any light condition.

STN7 abundance is regulated according to light conditions. Exposure of plants to far red (FR) light or HL has been shown to lead to decreased amounts of the STN7 kinase protein (Willig *et al.*, 2011; Wunder *et al.*, 2013). Exposure of plants to FR or HL likewise led to downregulation of *STN7* transcripts, demonstrating that STN7 is regulated also at the transcriptional level in a redox-dependent manner (Wunder *et al.*, 2013). The amount of the STN7 protein is up-regulated in Arabidopsis mutants devoid of PSI subunits and thus having the electron transfer chain (ETC) more reduced than in wild type (WT), whereas in the *tap38* mutant, with oxidized ETC., STN7 is down-regulated (Wunder *et al.*, 2013). The redox-state of the lumenal Cys residues has been shown to regulate *Chlamydomonas* Stt7 activity (Lemeille *et al.*, 2009). In higher plants, STN7 activity was shown to become inhibited at HL as well as with the DTT treatment implying that reduction of the Cys residues inhibits the kinase activity of STN7 (Rintamaki *et al.*, 2000). Also, transient dimerization of STN7 has been proposed to be connected with its kinase activity (Wunder *et al.*, 2013).

STN7 kinase has been shown to possess four phosphosites at its C-terminus (Reiland *et al.*, 2009) (Figure 1). Site-directed mutagenesis, replacing all four phosphorylated amino acids [three threonines (Thr) and one serine (Ser)] simultaneously by either alanine or aspartic acid suggested that STN7 phosphorylation is not essential for the function of the kinase, based on the fact that all mutants were capable of LHCII phosphorylation (Willig *et al.*, 2011). It was suggested that STN7 phosphorylation is rather linked to protein stability, as the phosphomimic mutants did not show degradation of the STN7 protein upon exposure to FR or blue light (Willig *et al.*, 2011). Enzymes and processes involved in regulation of the phosphosites in STN7 have remained elusive and the only fact reported is that STN8 kinase is not responsible for phosphorylation of STN7 (Reiland *et al.*, 2011). Furthermore, it is not known whether the different STN7 phosphosites have unique functions and regulations.

Here, we report a distinct difference between phosphorylation of the Thr and Ser residues of STN7 upon dark–light cycle. By applying targeted proteomics, we demonstrate that phosphorylation of the STN7 Thr-537 and Thr-541 residues decreases with increasing light intensity or when FR light alone is applied on active STN7 kinase, being tightly associated with STN7 degradation. On the contrary, the phosphorylation of the Ser-526 residue of STN7 coincides with phosphorylation of the client protein LHCII.

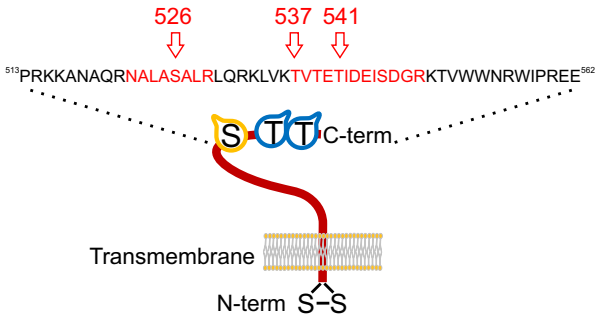

Figure 1. Three amino acid residues in the C-terminus of the STN7 kinase can be reversibly phosphorylated.
Schematic structure of the STN7 kinase showing the transmembrane domain, the disulphide bridge in the N-terminus protruding in the lumen, and the C-terminal phosphorylated residues Ser-526, Thr-537 and Thr-541. Also shown are the amino acid sequence of the STN7 C-terminal domain and the two tryptic peptides (in red) that bear the phosphorylations.

RESULTS

Degradation of the STN7 kinase under different illumination conditions

We first addressed the abundance of the STN7 kinase in the thylakoid membrane, as affected by illumination of WT Arabidopsis plants with FR light that predominantly excites PSI, with R light (RL) exciting mainly PSII and with HL that leads to inhibition of LHCII phosphorylation in the thylakoid membrane. To this end, WT plants were kept overnight in darkness (D) and in the morning at low light (LL) for 2 h to activate the STN7 kinase, followed by a treatment of plants under far red light (FRL) and RL for 2 h (Figure 2a), or under HL for 2, (HL2), 4 (HL4) and 6 h (HL6) (Figure 2b). In both experiments, light treatments were followed by thylakoid isolation and immunodetection of STN7 by western blot with two antibodies from different sources. Marked degradation of STN7 was evident with both antibodies (Figures 2 and S1a) after 2 h of FRL as well as upon treatment of plants with HL. Importantly, the degradation of STN7 was much faster in FRL than in HL, evidenced by degradation after 2 h of FRL being comparable to that observed in HL6. As expected, 2 h of FRL also led to complete dephosphorylation of the client LHCII proteins, detected with a phosphothreonine (P-Thr) antibody, while RL treatment had the opposite effect (Figure 2a).

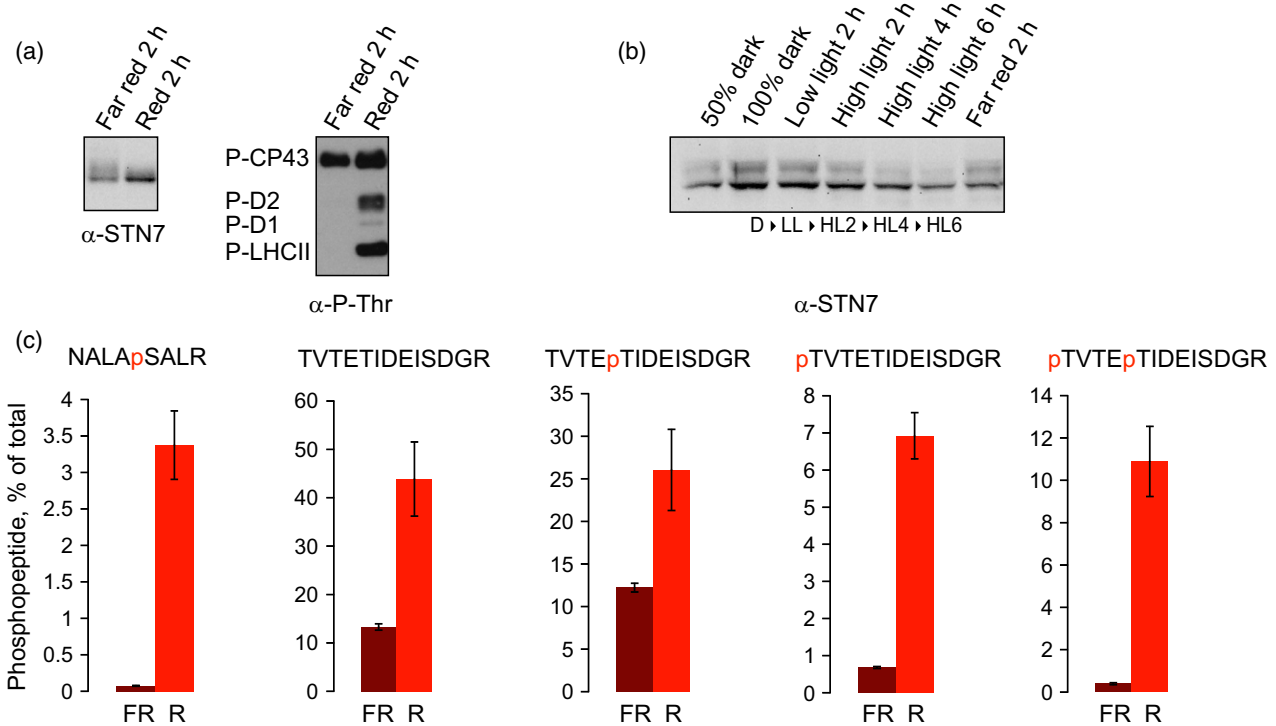

Figure 2. Changes in the amount and the phosphorylation status of the STN7 kinase upon exposure of Arabidopsis leaves to different qualities and quantities of light.
(a) Thylakoids were isolated from plants first acclimated to low light and subsequently treated with far red or red light for 2 h. Immunoblot (to the left) demonstrates the amount of the STN7 protein and the P-Thr immunoblot (to the right) demonstrates the relative changes in the phosphorylation status of PSII core phosphoproteins (P-CP43, P-D2, P-D1) and the LHCII (P-LHCII) proteins upon illumination of leaves with red and far red light.
(b) Thylakoids were isolated from plants acclimated to darkness (D), and subsequently treated first with low light for 2 h (LL), and next with high light for 2 h (HL2), 4 h (HL4) and 6 h (HL6), or with far red light for 2 h. Immunoblot demonstrates the changes in the amount of the STN7 kinase upon the light treatments.
(c) Thylakoids were isolated from plants first acclimated to low light and subsequently treated with far red (FR) or red (R) light for 2 h, followed by fractionation of the proteins with SDS-PAGE and relative quantification by SRM of the different phosphorylation sites of the STN7 kinase. From left to the right: relative Ser-526 phosphorylation in FR and R; all single and double Thr phosphorylations summed up; phosphorylation of Thr-541 residue (TVTEpTIDEISDGR); phosphorylation of Thr-537 residue (pTVTETIDEISDGR) and both Thr-541 and Thr-537 residues (pTVTEpTIDEISDGR). Data are presented as means ± standard deviation (SD) of three biological replicates with two technical replicates.

Arabidopsis STN7 has one Ser and two Thr phosphosites – behaviour under RL and FRL

Next, the phosphorylation status of the STN7 kinase (Willig *et al.*, 2011) was investigated in plants treated with different light conditions. To this end, a targeted proteomics method was set up. Thylakoid proteins were first separated by SDS-PAGE, the band corresponding to STN7 was localized (Figure S1b) and finally in-gel digested with trypsin (Table S1). The phosphopeptides identified were then quantified in relative terms by means of selected reaction monitoring (SRM) (see Experimental Procedures and Tables S2 and S3) (Jin *et al.*, 2010; Konert *et al.*, 2015). Plants treated with RL and FRL, with the most striking difference in the abundance of STN7 (Figure 2a), were the first ones submitted to SRM analysis. The peptide signals detected were confirmed to be the targeted phosphopeptides by digesting, as a negative control, the band with the same molecular mass from *stn7* plants treated with similar light conditions (Figure S2a–l).

The peptide bearing the Ser phosphosite (NALA-S^{526}ALR) was detected only in two forms (nonphosphorylated and phosphorylated), and the phosphoform (NALApSALR) was present in plants treated with RL (PSII light) but missing from FRL (PSI light) treated plants. Summing up the four most intense transitions of each form from RL treatment, it was possible to estimate that NALApSALR was about 4% of the total intensity of the NALASALR peptides (Figure 2c and Table S3). In contrast, the tryptic peptide $T^{537}VT^{539}ET^{541}$IDEISDGR was found in several forms (Table S2). Besides the nonphosphorylated and phosphorylated forms, it was found as mis-cleaved peptides on both the N-terminus (LVKTVTETIDEISDGR) and the C-terminus (TVTETIDEISDGRK). The C-terminus ragged end peptide (TVTETIDEISDGRK) was also the most flyable, both as non-phosphorylated form and as TVTEpTIDEISDGRK. Through the spectra obtained in data-dependent acquisition (DDA), it was possible to determine which of the three Thr residues was

phosphorylated from all the singly phosphorylated forms except for LVKTVTETIDEISDGR. However, according to phosphoRS analysis (Taus *et al.*, 2011) of the phosphopeptides detected (Table S2), none of these forms was found to be phosphorylated on Thr 539. Furthermore, no peptides were found with all the three Thr residues phosphorylated simultaneously. In the case of LVKTVTETIDEISDGR, the detection in SRM of a signal for the transition b5-98 (neutral loss) that corresponds to phosphorylation on Thr-537 (Figure S2k, on the right), but not for transitions y9 and y9-98 that would correspond to phosphorylation on Thr-541 (Figure S2k, on the left), brought to assignment of phosphorylation on the first Thr (Thr-537). For the phosphopeptide TVTEpTIDEISDGR, the signal of the transition b2 excludes the phosphorylation on Thr-537, while the signal of the transition y9-98 confirms the phosphorylation on Thr-541 (Figure S2l, upper on the left). The same is observed for the phosphopeptide TVTEpTIDEISDGRK with the signals for transitions b2 and $y10^{2+}$-98, respectively (Figure S2l, upper on the right). In the case of the doubly phosphorylated peptide pTVTEpTIDEISDGRK, the signal of the transition y10-98 indicates the phosphorylation on Thr-541, while the signal of the transition $y12^{2+}$-98 excludes the phosphorylation on Thr-539 (Figure S2l, lower on the left). Finally, for the doubly phosphorylated peptide LVKpTVTEpTIDEISDGR, the signals of the transitions b4-98 and b5-98 indicate phosphorylation on Thr-537, while the signal of the transition y9-98 excludes the phosphorylation on Thr-539. For the phosphopeptide pTVTETIDEISDGRK, besides the signal for the transition y10, it was not possible to use a transition to discriminate between Thr-537 and 539 (Figure S2g), so the phosphorylation was assigned to Thr-537 on the basis of the phosphoRS analysis (Table S2). The four most intense transitions of every form of the peptide TVTETIDEISDGR, including the missed cleavage forms, were summed up, and the contribution of every form to the total was calculated as percentage with the formula described in Experimental Procedures. Every phosphorylated form (pTVTETIDEISDGR, TVTEpTIDEISDGR or pTVTEpTIDEISDGR) was calculated as a separate phospho-species. The sum of all Thr phosphoforms is shown in Figure 2(c) (second graph to the left) and the results for each individual Thr phosphopeptide are presented in the right part of Figure 2(c). All the three phosphoforms of TVTETIDEISDGR were found to be rather high in plants treated with RL. In particular, the phosphorylation on Thr-541 was relatively most abundant, reaching 25% of the total in RL-treated plants. Notably, this was the only phosphoform detectable in relatively high amounts also in FRL-treated plants. The sum of the three Thr phosphoforms was over 40% of the total in RL-treated plants whereas in FRL it was only about 10%.

Ser 526 phosphorylation is differentially regulated with respect to Thr under white light

To assess whether the Ser-526, Thr-537 and Thr-541 phosphorylations are connected either to degradation or to the activity of STN7, plants grown under 8 h photoperiod were sampled at given time points during a dark–white light–dark cycle. Dark-acclimated plants were sampled after 16 h of D (D1), followed by 2 h of LL (LL1) and then by 2 h of HL, like in the experiment in Figure 2(b), but two further samplings were included; after another 2 h of LL (LL2) and after subsequent 16 h of D (D2). As shown in the western blot with the P-Thr antibody (Figure 3a) only the LL treatments, after either D or HL, induced clear phosphorylation of the client protein LHCII (also minor phosphorylation after D1). Analysis of relative phosphorylation level of the STN7 phosphosites from the same samples gave an unexpected result: similar to LHCII phosphorylation, only LL induced significant increase in the relative phosphorylation of Ser-526 in STN7 (Figure 3b). However, the percentage of phosphorylation of Ser-526 after LL was significantly less than that observed after treatment with RL only (Figure 2c). Notably, the increase/decrease in the Ser-526 phosphorylation did not correlate with degradation of the STN7 protein, as explained in the technical note in the Experimental Procedures (Figure S3). Instead, phosphorylation of the Thr residues decreased with increasing light intensity (Figure 3c). The highest phosphorylation level was found in D-acclimated samples, both at the beginning and at the end of the white light cycle, the lowest level occurred in HL, while in LL1 and LL2 the phosphorylation of the Thr residues was in between those in D and HL (Figure 3c). Noteworthy, treatment of plants with LL significantly decreased Thr-541 phosphorylation, which is the dominant phosphoform in STN7 (Figure S4a), the decrease being similar both in LL1 and LL2, thus independent of the previous light conditions. The pTVTETIDEISDGR form, instead, reached the highest level in LL2, after the HL treatment had induced marked decrease of TVTEpTIDEISDGR and pTVTEpTIDEISDGR.

Taken together, the level of Thr phosphorylation in STN7 after the dark treatment of plants was comparable to that found in RL-treated plants. In contrast, Ser-526 phosphorylation was induced only by LL (Figure 3b), in addition to the RL treatment (Figure 2c). Yet, none of the white light conditions was capable of inducing the phosphorylation of either the Ser or Thr phosphosites to as high level as observed upon RL illumination.

STN7 phosphorylation in the tap38 and pbcp phosphatase mutants under white light-dark cycles

To get further insights into the role of differential phosphorylation of STN7 phosphosites in the function and turnover of STN7, the light–dark cycle used for WT plants

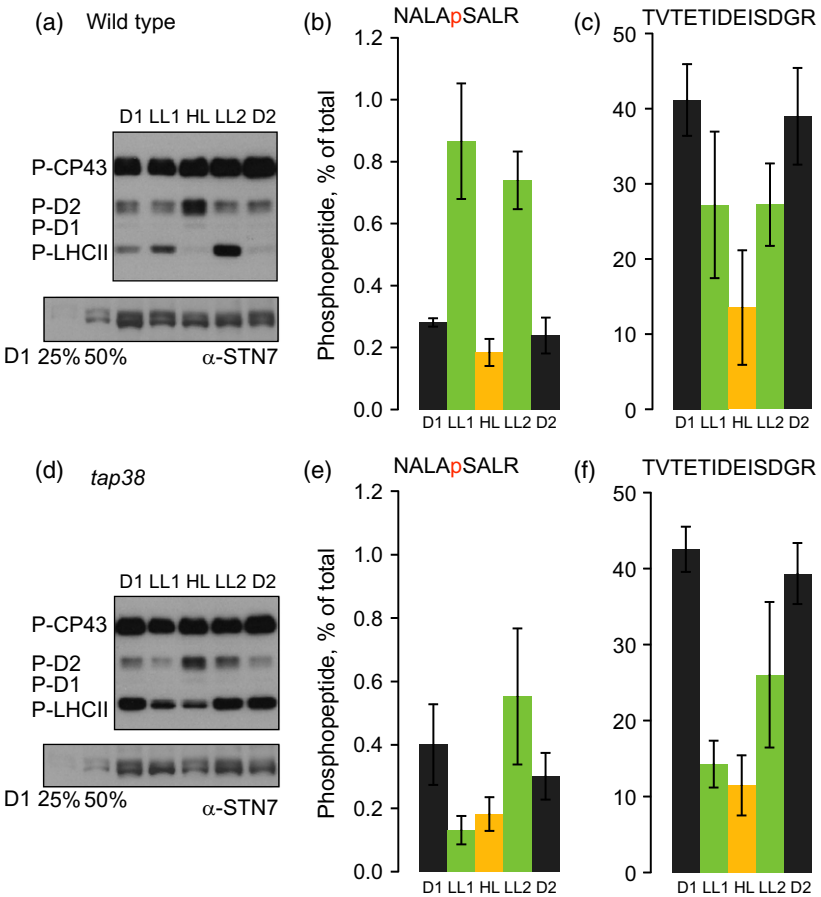

Figure 3. Relationship between the phosphorylation status of the PSII core and LHCII proteins, the amount of the STN7 kinase and the phosphorylation of the STN7 kinase Thr and Ser residues in the WT and *tap38* mutant plants upon exposure to varying light conditions.
Thylakoids were isolated from plants in the end of overnight exposure to darkness (D1), then shifted to low light for 2 h, (LL1), next to high light for 2 h (HL), again to low light for 2 h (LL2) and finally to darkness overnight (D2).
(a, d) P-Thr immunoblot demonstrating the changes in PSII core (P-CP43, P-D2, P-D1) and LHCII (P-LHCII) protein phosphorylations (above) and in the amount of the STN7 kinase (below) in WT (a) and *tap38* (d) plants upon changing light conditions. Here, 25 and 50% denote for the amount of the sample loaded on side of the 100% samples to demonstrate the linear immunoresponse of the STN7 antibody.
(b, e) Relative SRM quantification of Ser-526 phosphorylation of the STN7 protein in differentially light treated WT (b), and *tap38* (e) plants. Data are presented as means ± standard deviation (SD) from four biological and two technical replicates.
(c, f) Relative SRM quantification of all STN7 phosphopeptides containing single or double Thr phosphorylation (represented as sum) in differentially light treated WT (c) and *tap38* plants (f). Data are presented as means ± SD from four biological and two technical replicates.

(Figure 3a–c) was applied also to the *tap38* (Figures 3d–f and S4b) and *pbcp* mutant plants (Figure S4c,d). The *pbcp* plants did not show any major difference in the dynamics of STN7 phosphorylation as compared to WT (Figure S4c), indicating that PHOTOSYSTEM II CORE PHOSPHATASE (PBCP) is not directly connected to regulation of STN7 phosphorylation in the light conditions tested here, and therefore were not further considered here.

Instead, the STN7 Ser-526 phosphorylation in *tap38* plants differed from that of WT in showing no distinct induction of phosphorylation upon the first white light treatment (LL1). Only the second white light treatment, LL2 after HL, induced Ser-526 phosphorylation typical for WT plants in LL (Figure 3e). STN7 Thr phosphorylation, conversely, showed in all light treatments the same trends observed in WT. Dephosphorylation of STN7 Thr residues occurred with increasing light intensity, although in the case of *tap38*, Thr phosphorylation in LL1 was as low as in HL (Figure 3f), especially concerning the doubly phosphorylated peptide pTVTEpTIDEISDGR, (Figure S4b). After very low Thr phosphorylation of STN7 in HL, the exposure of plants to LL2 and D2 brought back the higher Thr phosphorylation.

The abundance of STN7 in the thylakoid membrane was also affected by various light-dark treatments of the *tap38* plants (Figure 3d, western blot lower panel). Already in dark-acclimated plants the level of STN7 was lower compared to WT. This data was confirmed by SRM, using whole thylakoids of dark-adapted WT, *tap38* and *stn7* plants digested by trypsin in the stacking gel and using the two core subunits of PSI (PsaA and PsaB) as a stable reference. The three most intense transitions of the three most intense peptides of each protein, STN7, PsaA and PsaB, were summed up and the results were used to calculate the relative ratio between STN7 and each of the two PSI subunits (Figure S5a and Table S3). Obtained results for all three genotypes showed unaffected ratio between the two core PSI subunits (PsaA/PsaB), whereas the ratios PsaA/STN7 and PsaB/STN7 were significantly higher in *tap38* than in WT, in line with the results obtained with western blotting (Figure S5a).

Interestingly, even though the abundance of the STN7 client proteins Lhcb1 and Lhcb2 remained stable throughout the light treatments (Figure S5b), the phosphorylation levels of Lhcb1 and Lhcb2 decreased in the *tap38* mutant plants upon transfer from D to LL1 (Figure 3d), the LHCII

phosphorylation status thus following that of Ser-526 phosphorylation.

STN7 phosphorylation and degradation in WT and tap38 upon transfer of plants from darkness directly to RL and FRL

To get more detailed insights into the mechanism of STN7 activation in phosphorylation of the client LHCII proteins, the dark-acclimated WT and *tap38* plants were directly illuminated with FRL and RL, and sampled from each condition after 1, 10 and 120 min (Figure 4). As shown in Figure 4b, Ser-526 phosphorylation increased in WT in the time course of RL illumination, in accordance with phosphorylation of the STN7 client protein LHCII. The *tap38* plants behaved similarly to WT: illumination by RL was likewise efficient in increasing Ser-526 phosphorylation and concomitantly an increase in LHCII phosphorylation took place.

In line with similar Ser phosphorylation in *tap38* and WT, the Thr phosphorylations of STN7 also behaved similarly in WT and *tap38* plants upon RL and FRL illumination (Figure 4c). Despite strong dephosphorylation of the Thr residues upon two-hour treatment with FRL, applied directly after D, no significant degradation of STN7 occurred in WT or *tap38* (Figure 4a, lower panel). This provided compelling evidence that the FRL *per se* is not decisive in causing the fast degradation of the STN7 kinase but it rather depends on the pre-condition, i.e. the activation state of STN7 upon pre-illumination period (Aro and Ohad, 2003). Furthermore, 120 min of FRL brought to complete dephosphorylation of LHCII in *tap38*, thus occurring in the absence of the TAP38 phosphatase (Figure 4a, upper panel) and indicating that some other, yet uncharacterized, phosphatase(s) acts redundantly on P-Thr of LHCII.

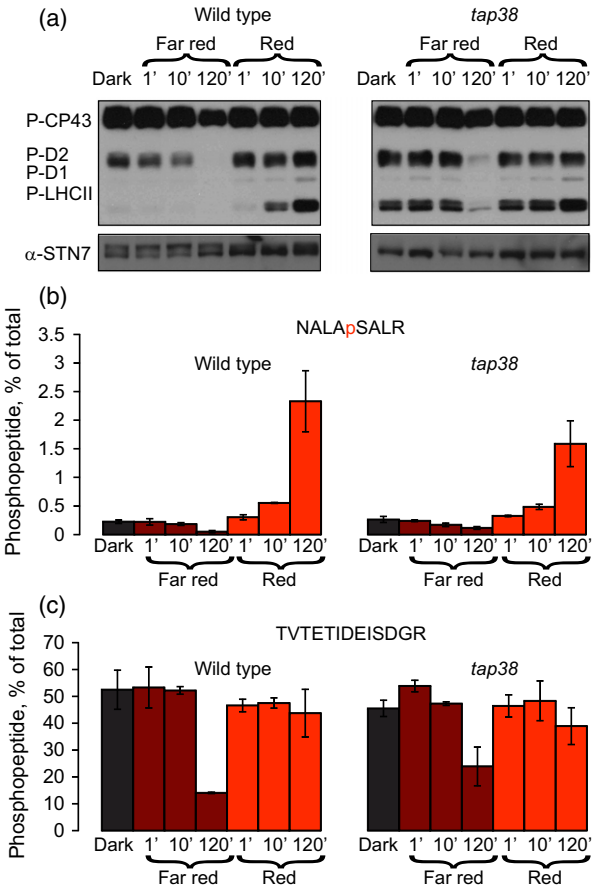

Figure 4. PSII core and LHCII protein phosphorylation, amount of the STN7 kinase and phosphorylation of the STN7 kinase Thr and Ser residues in WT and *tap38* plants in response to varying light qualities.
WT and *tap38* plants were kept under darkness for 16 h and subsequently exposed to far red and red light for one, 10 and 120 min.
(a) P-Thr immunoblot demonstrating relative changes in PSII core (P-CP43, P-D2, P-D1) and LHCII (P-LHCII) phosphoproteins (on the top), and in the amount of the STN7 kinase (below) in the course of illumination of WT (left) and *tap38* (right) plants with far red and red light.
(b, c) Relative SRM quantification of (b) the Ser-526 phosphorylation and (c) single or double Thr phosphorylations (represented as sum) of the STN7 kinase. Data are presented as means ± standard deviation (SD) from three biological and two technical replicates.

DISCUSSION

During the past few years, technical progress in mass spectrometry has allowed important improvements in elucidation of the role of PTMs in regulation of chloroplast proteins (Buren *et al.*, 2011; Alban *et al.*, 2014; Lehtimaki *et al.*, 2015; Mazzoleni *et al.*, 2015). Here, we applied a targeted approach to relatively quantify single phosphosites of a low-abundant membrane protein, the STN7 kinase, without using phosphopeptide enrichment. Even though our method does not allow direct estimation of the absolute phosphorylation of STN7 in distinct phosphosites, it nonetheless avoids several passages – and thus potential technical pitfalls – required to enrich phosphopeptides in a sample (Kauko *et al.*, 2015). Thus, the method allowed observation of subtle changes occurring in distinct phosphosites of the STN7 kinase upon various light treatments and in different genotypes, and an assignment of the functional role for these phosphosites in the activity and degradation of the STN7 kinase.

The Stt7 kinase of *Chlamydomonas* and its homologue STN7 in Arabidopsis have previously been shown to be phosphorylated on Thr and Ser residues (Figure 1) (Lemeille *et al.*, 2010; Reiland *et al.*, 2011). The kinase protein catalyzing the STN7 phosphorylation has remained elusive, as it has only been shown STN8 is not responsible for the phosphorylation of STN7 (Reiland *et al.*, 2011). Furthermore, it is also possible that STN7 becomes autophosphorylated. Phosphorylation of the Ser-533 residue in the C-terminal domain of the Stt7 kinase was shown not be linked to the function of the kinase, as the *Chlamydomonas* strain with a S533D/A change was still able to phosphorylate LHCII under RL illumination (Lemeille *et al.*, 2010).

However, the C-terminal domains of Stt7 and STN7 are not conserved (Willig *et al.*, 2011), leaving the question on the functional role of Ser-526 phosphorylation in the STN7 kinase to be answered. The second question addressed here concerns the specific roles of phosphorylation of the Ser and Thr residues in protection of the STN7 kinase against degradation (Willig *et al.*, 2011). Yet the third unresolved problem was addressed: how the artificial light conditions, generally used to induce 'state transitions' in experimental conditions (e.g. Brautigam *et al.*, 2009), affect the phosphorylation of the STN7 kinase and how they differ from those induced by changes in white light intensity occurring in natural environments, where plants use reversible LHCII phosphorylation to avoid 'state transitions' (Mekala *et al.*, 2015). Additionally, a multiphase light treatment series (D1-LL1-HL-LL2-D2) was applied in order to address the possible role of the preceding light conditions for LL-induced phosphorylation of LHCII.

Ser-526 phosphorylation is coupled to STN7 activity in phosphorylation of the LHCII proteins, whilst phosphorylation of the Thr residues protects STN7 against degradation

Thanks to the possibility of monitoring the single phosphosites instead of studying all of them together (Willig *et al.*, 2011), we demonstrate here that the Ser-526 phosphorylation of STN7 is coupled to its activity in phosphorylating the LHCII proteins. Although it is not possible to state whether the Ser phosphorylation in STN7 directly induces the kinase activity, the phosphorylated Ser-526 present in the STN7 kinase yet directly correlates with the client protein LHCII phosphorylation, in WT maximally occurring under RL, to somewhat lesser extent in LL and being practically absent under HL and D conditions (Figures 2, 3 and 4). However, when it comes to Ser-526 and LHCII phosphorylation upon the D1-LL1-HL-LL2-D2 cycle, the possibility of natural circadian rhythm simultaneously affecting both of these phenomena cannot be disregarded.

In addition to the WT, the *tap38* mutant also turned out to be a relevant tool to address the functional role of Ser-526. Unlike in WT, the lack of the LHCII phosphatase in *tap38* allows direct estimation of the role of STN7 Ser-526 phosphorylation (assessed by SRM) on the client LHCII protein phosphorylation (assessed by P-Thr immunoblotting of thylakoid proteins). Indeed, despite a still unexplained decrease in LHCII phosphorylation in *tap38* upon a shift of plants from D to LL1 (Figure 3) (see below), the subsequent induction of LHCII phosphorylation, particularly upon a shift of plants to LL2, induced a clear phosphorylation of the client LHCII proteins with concomitant increase in Ser-526 phosphorylation of the STN7 kinase. Similar relationship was evident under unnatural RL and FRL illumination conditions that are historically known to induce reversible 'state transitions' (Figure 4). Thus, even though the *tap38* mutant has less STN7 in their thylakoid membrane compared to WT (Figures 3d and S5a, and Wunder *et al.*, 2013) the dynamics of the STN7 kinase activity nevertheless resembles that observed in WT (Figures 3 and 4) and the *pbcp* mutant (Figure S4c).

It has previously been demonstrated that STN7 has a high turnover rate and that particularly the FRL illumination is efficient in inducing the degradation of STN7 (Willig *et al.*, 2011; Wunder *et al.*, 2013). Our analyses confirmed the FRL induces STN7 degradation. Importantly, it was possible to assign the dephosphorylation of the two Thr residues, Thr-537 and Thr-541, as essential pre-conditioning for the degradation of the STN7 kinase. Moreover, the consequences of more natural white light–dark cycles on the stability and degradation of the STN7 kinase were investigated. Clearly, the HL conditions provoke the degradation of STN7 and marked dephosphorylation of its two Thr residues is evident in HL in both WT and *tap38* (Figures 2 and 3), although the degradation occurs more slowly than upon FRL illumination.

In contrast, the stability of STN7, occurring particularly in darkness, was accompanied by strong phosphorylation of the Thr-537 and Thr-541 residues of STN7.

Activation of both the STN7 kinase and LHCII phosphorylation are strongly dependent on pre-illumination of plants – physiological implications

The STN7 kinase can exist either in an activated (RL, LL), deactivated (D) or inhibited (HL) state, depending on the chloroplast redox environment (Aro and Ohad, 2003). Furthermore, under white light conditions the phosphorylation of the two major LHCII proteins, Lhcb1 and Lhcb2, by the STN7 kinase is known to be maximal under relatively LL intensities, lower than those previously experienced by a plant during the growth (Rintamaki *et al.*, 1997; Pesaresi *et al.*, 2009; Mekala *et al.*, 2015; Suorsa *et al.*, 2015). Here we specifically addressed the role of the pre-illumination condition on phosphorylation of the STN7 kinase and its target LHCII proteins. Thus, a multiphase treatment of plants with white lights of different intensity (D1–LL1–HL–LL2–D2) was applied to investigate the causal relationships between the plant pre-treatment condition and the subsequent capacity of the following illumination condition to phosphorylate/dephosphorylate the STN7 kinase phosphosites as well as the LHCII client proteins.

Intriguingly, LL2 induced clearly higher phosphorylation level of LHCII than LL1 (Figures 3 and S4c). Thus the HL illumination that inhibits the STN7 kinase and LHCII phosphorylation (Aro and Ohad, 2003), is a less serious pre-treatment for subsequent LL activation of the STN7 kinase than the dark incubation of plants with deactivation of the STN7 kinase (Aro and Ohad, 2003). Further, whereas the comparison of the behavior of the *tap38* mutant in unnatural RL/FRL illuminations did not reveal much difference to

that of WT (Figure 4), the more natural dark–white light shifts demonstrated an anomalous and rather unexpected behavior of the *tap38* mutant as compared to WT. Despite the absence of the LHCII specific TAP38 phosphatase, the LHCII phosphorylation level was not stable in *tap38*, instead, dephosphorylation of LHCII upon D1–LL1 shift and even more markedly upon LL1–HL shift was evident (Figure 3; Rantala *et al.*, 2016). This result not only indicates that another, yet uncharacterized phosphatase(s) likely exists, but it also provides compelling evidence that even in the absence of the counteracting TAP38 phosphatase, the phosphorylation level of LHCII is dictated by the phosphorylation of the Ser-526 of STN7. An interesting feature was that in *tap38*, the STN7 kinase appeared to be deactivated upon the first LL treatment (LL1), which strongly coincided with a very low Ser-526 phosphorylation in STN7.

Taken together, the data demonstrated here provide fundamental insights into the regulation of LHCII protein phosphorylation by the STN7 kinase, as summarized in Figure 5. Considering the 'state transition' lights, RL induces a high phosphorylation status of STN7 Ser-526 (Figures 2 and 4) which is not reached in any white light condition tested (Figure 3) whereas FRL rapidly degrades the STN7 kinase via dephosphorylation of the Thr residues of STN7 (Figure 2). Nonetheless, the complex 'regulation of the regulator' under natural environmental conditions cannot be dissected by subjecting the plants only to artificial light qualities (RL and FRL). Indeed, the observed effects of fluctuating white light–dark cycles, and the preceding light condition, on STN7 phosphorylations in the C-terminus and via that, on LHCII phosphorylation in the thylakoid membrane demonstrate that regulation of LHCII phosphorylation is more dynamic and complicatedly regulated process than previously understood. As natural light conditions are characterized by immense and abrupt fluctuations in light intensity, the STN7 phosphorylations and dephosphorylations at distinct sites are likely to bear a fundamental role for plant acclimation according to environmental cues. It is noteworthy that under natural light conditions, plants actively avoid state transitions upon shifts between LL, HL and D (Mekala *et al.*, 2015), using reversible LHCII phosphorylation as a tool, via activation/deactivation and degradation of the STN7 kinase.

EXPERIMENTAL PROCEDURES

Plant material and growth conditions

Arabidopsis thaliana ecotype Columbia WT as well as the *tap38* (Pribil *et al.*, 2010; Shapiguzov *et al.*, 2010) *pbcp* (Samol *et al.*, 2012) and *stn7* (Bellafiore *et al.*, 2005) mutants were used for experiments. The plants were grown in a mixture of soil and vermiculite (1:1) at 23°C under 120 μmol photons m^{-2} sec^{-1} of light with a photoperiod of 8 h light and 16 h dark, OSRAM PowerStar (Munich, Germany) HQIT 400/D Metal Halide lamps as the light source. Five-week-old plants were used for all experiments.

Light treatments

Noteworthy, the light treatments were performed with entire intact plants, not with detached leaves. The plants were treated with darkness, LL (20 μmol photons m^{-2} sec^{-1}) or HL (1000 μmol photons m^{-2} sec^{-1}), or with R and FR lights (Piippo *et al.*, 2006). The temperature was controlled during all treatments not to exceed 23°C.

Isolation of the thylakoid proteins and western blotting

Thylakoid membranes were isolated essentially as described in (Jarvi *et al.*, 2011), with all buffers supplemented with 10 mM NaF. The chlorophyll (Chl) content was measured according to (Porra *et al.*, 1989). Thylakoids were solubilized according to (Laemmli, 1970) and separated by using SDS-PAGE (12% (w/v) polyacrylamide, 6 M urea), the gels loaded based on an equal chlorophyll concentration. After electrophoresis, the proteins were either electroblotted to a polyvinylidene fluoride (PVDF) membrane, or processed for mass spectrometry. The membranes were probed with a P-Thr (New England Biolabs, Ipswich, MA, USA), or with antibodies raised against STN7 (Agrisera, www.agrisera.com, catalogue number AS101611 or a gift from prof. Roberto Barbato), Lhcb1 or Lhcb2 (Agrisera catalogue numbers AS09 522 and AS01 003, respectively). Horseradish peroxidase-linked secondary antibody and enhanced chemiluminescence reagents (Amersham, GE Healthcare, Pollards Wood, UK) were used for detection.

Detection of STN7 phosphorylation and relative quantitation

Separation of thylakoid proteins in SDS-PAGE and identification of the STN7 band. Thylakoids corresponding to 3 μg of Chl were solubilized (Laemmli, 1970), run for 0.5 cm in a 6% acrylamide, 6 M urea SDS-PAGE (stacking gel) to become denatured and purified, and subsequently subjected to in-gel digestion with a sequencing grade modified trypsin (Promega V5111, Madison, WI, USA). To be able to enrich STN7 and consequently detect phosphopeptides, a method to identify the band containing STN7 in SDS-PAGE was used as in (Konert *et al.*, 2015). WT thylakoid preparations corresponding to 10 μg of Chl from D and LL treatments were separated in a 20 cm 12% acrylamide 6 M urea SDS-PAGE (PROTEAN II xi Cell, Bio-Rad, Hercules, CA, USA), partially transferred onto a PVDF membrane for 15 min with a TE77XP Semi-Dry Transfer Unit (Hoefer, Holliston, MA, USA) followed by immunodecoration with the STN7 antibody (Agrisera, catalogue number AS10 1611, Vännäs, Sweden). Thylakoids from the *stn7* plants treated with LL were used as control. The partially transferred gel was stained with Coomassie Brilliant Blue (0.1% w/v Coomassie stain, 40% ethanol, 10% acetic acid), and the exact position of the STN7 band was identified by overlapping the antibody signal with both the image of the gel and of the PVDF membrane stained with Coomassie blue (Figure S1b). The corresponding band in this gel, as well in samples from different treatments in following gels, was digested with trypsin as described above.

Analysis by LC-ESI-MS/MS

The eluted peptides of both whole thylakoids and the identified STN7 band were analyzed in DDA mode with Q-Exactive, an ESI-hybrid quadrupole-orbitrap mass spectrometer (Thermo Scientific, Thermo Fisher Scientific, Waltham, MA, USA) as described previously (Konert *et al.*, 2015). Dried peptides were resuspended in 2% formic acid, spiked with iRT peptides according to

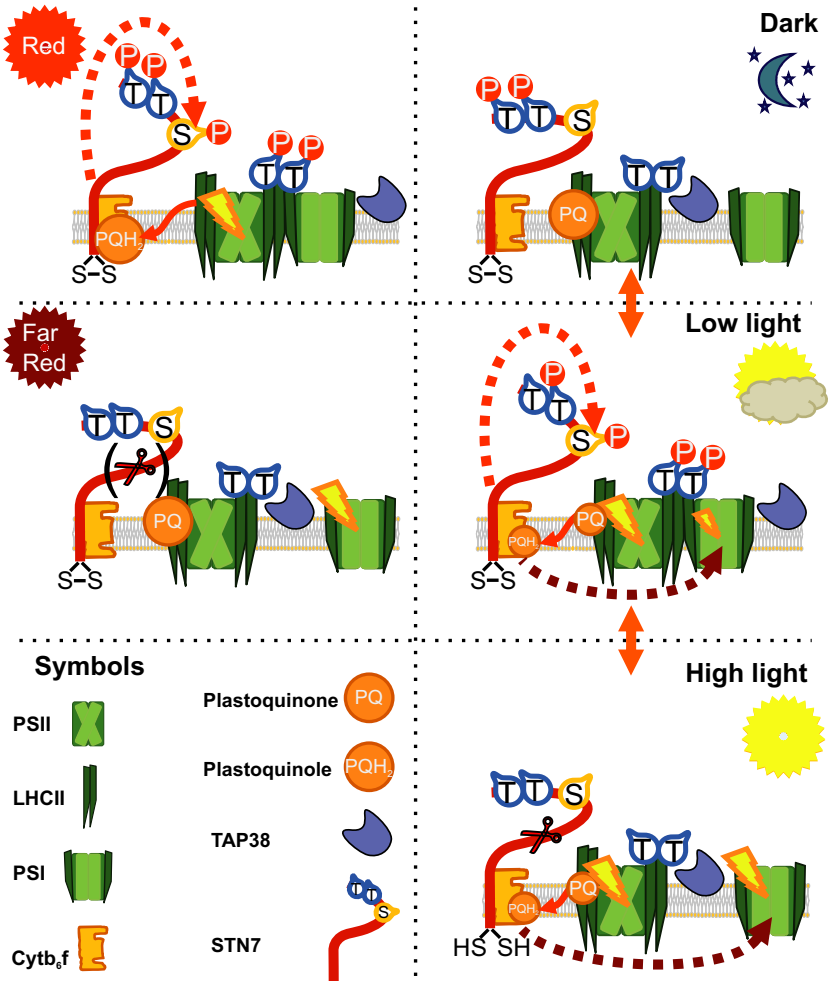

Figure 5. Schematic representation of the role of STN7 kinase phosphorylation, dephosphorylation and degradation in modulation of the target LHCII protein phosphorylation.
Response of STN7 phosphorylation to the treatment of plants with red and far red light distinctly differs from that obtained by treatment of plants with varying intensities of white light. Red light (upper left corner) induces maximal phosphorylation of both the Ser-526 and Thr residues of the STN7 kinase. Ser-526 phosphorylation coincides with a maximal phosphorylation of the target protein LHCII, whereas phosphorylation of the Thr residues prevents degradation of the kinase. Illumination with far red light (middle left), in contrast, leads to dephosphorylation of the STN7 Thr residues, resulting in its degradation. Ser-526 of the STN7 kinase becomes likewise dephosphorylated upon illumination with far red light, as also the target LHCII proteins. Treatment of plants with different intensities of white light is depicted on the right hand side. In darkness, when the target LHCII proteins are dephosphorylated, the Ser residue is likewise dephosphorylated but the Thr residues are maximally phosphorylated like under red light. The Ser residue of STN7 is phosphorylated only under low light concomitantly with prominent phosphorylation of the target LHCII proteins. Subsequent high light treatment leads to almost complete dephosphorylation of both the Ser and Thr residues of the STN7 kinase, coinciding with the loss of STN7 activity and the degradation of the STN7 kinase. Broken red line indicates the condition when light-induced phosphorylation of the Ser-526 residue in STN7 is possible and as a consequence, via phosphorylation of the LHCII antenna, allows the balanced excitation energy distribution between the two photosystems. Broken brown line indicates electron flow from *Cytb$_6$f* to PSI, which occurs only in white light.

manufacturer's instructions (Biognosys, Zürich, Switzerland) and loaded in a nanoflow HPLC system (EasyNanoLC 1000, Thermo Fisher Scientific) coupled to the Q-Exactive (Thermo Scientific) mass spectrometer equipped with a nano-electrospray ionization source. The mobile phase consisted of water/ACN (98:2 (v/v)) with 0.2% FA (v/v) (solvent A) or ACN/water (95:5 (v/v)) with 0.2% FA (v/v) (solvent B) at a flow rate of 300 nL min^{-1}. Peptide mixtures were separated by a two-step gradient elution from 2 to 35% solvent B in 40 min, followed by 5 min 35 to 100% and subsequently 10 min 100% solvent B. The scan range was set from 300 to 2000 m/z and the type of fragmentation used was HCD (Higher-energy collisional dissociation). Up to 10 data-dependent MS/MS spectra were acquired in each scan, with the dynamic exclusion set for 10 sec.

Data analysis and MS/MS spectra interpretation

MS/MS spectra were searched with an in-house Mascot (v.2.4) (Matrix Science, London, UK) search engine and analyzed using Proteome Discoverer (v.1.4) Software (Thermo Scientific) using as database the nonredundant Arabidopsis proteome (TAIR10, www.arabidopsis.org) supplemented with most common contaminants (in total 35502 entries). The search parameters were the followings: monoisotopic mass, one missed cleavage allowed, precursor mass tolerance 5 ppm, fragment mass tolerance 0.02 Da, m/z $\geq 2+$. The following modifications were included: carbamidomethylation of cysteine (static modifications) (mono $\Delta = 57.021464$), and, as variable modifications, oxidation of methionine,(mono $\Delta = 15.9949$), phosphorylation of serine, threonine and tyrosine (mono $\Delta = 79.9663$), de-amination of asparagine and glutamine (mono $\Delta = 0.98402$). Identifications of phosphopeptides and peptides were validated through PhosphoRS filter (version 3.1, Taus *et al.*, 2011) and Decoy Database Search, with target false discovery rates (FDR) of <0.01 (strict) and <0.05 (relaxed). For phosphopeptides the confidence threshold was set to $P < 0.05$.

To increase the probability of identification of phosphopeptides and verify the presence of previously undescribed PTMs, a list of masses corresponding to the tryptic peptides of STN7 was generated by means of in-silico digestion. The digestion was performed using the Skyline software, v. 3.1.0.7382 (MacLean *et al.*, 2010).The generated 'inclusion list' included the doubly and triply charged masses of all the tryptic peptides generated with a length between 6 and 25 amino acids and included the possibility of having missed cleavage both on N-terminus and C-terminus and three variable modifications among those described above. The MS/MS analysis was repeated by restricting the fragmentation to the generated masses only. No new PTMs were found, and all the phosphopeptides previously described in literature were detected (Table S2), indicated in red in Figure 1.

SRM analysis

The DDA search results, which included doubly and triply charged peptides with 1 miss-cleavage, were transferred to Skyline software to generate SRM transitions to the peptides listed in Table S3. A triple stage quadrupole TSQ Vantage QQQ mass spectrometer (Thermo Scientific, Thermo Fisher Scientific), quipped with the same nano-electrospray ion source used for Q-Exactive and in line with a similar nanoLC system, was utilized to perform SRM measurements. The gradient used was optimized to separate the target phosphopeptides, i.e. 10 to 35% solvent B in 20 min, followed by 35 to 100% in 2 min and 5 min of 100% solvent B with a flow rate of 300 nL min^{-1}. The mass spectrometer was operated in the positive ion mode with a capillary temperature of 270°C, spray voltage of + 1600 V and collision gas pressure of 1.2 mTorr. Measurements in scheduled mode were performed with a cycle time of 2 sec and a dwell time of ca. 10 msec, using a window of 3 min to allow maximum 100 concomitant transitions.

The raw mass spectrometry proteomics data from this work have been submitted to the PeptideAtlas database (http://www.peptideatlas.org/PASS/PASS00811) and assigned to identifier PASS00811. The refined SRM dataset can be accessed via https://panoramaweb.org/labkey/STN7_phosphosites_quantification.url.

Calculation of phosphorylation stoichiometry

STN7 appeared to be a relatively abundant protein in the identified gel band (Table S1), while in whole thylakoids, without separation in SDS-PAGE, only a few peptides could be detected. Indeed, although co-migration of STN7 with several other abundant proteins was evident, one of which was the highly abundant ATPase β-subunit, it was still possible to cover most of the STN7 protein and to find the phosphopeptides. It is important to note that it was impossible to detect and, consequently, to relatively quantify various STN7 phosphorylations from the whole thylakoids without a TiO_2 or IMAC phosphopeptide enrichment. TiO_2 enrichment, however, might not be the best choice when analyzing small differences due to an intrinsic bias introduced by the enrichment step (Kauko *et al.*, 2015). So, instead of enriching the phosphopeptides, we found it more convenient to 'enrich' the target protein through fractionation in SDS-PAGE. To estimate the phosphorylation stoichiometry of STN7 phosphosites, it was decided to calculate the differences in phosphorylation by measuring the intensities of the peptides and corresponding phosphopeptides, and eventually to express the amount of phosphorylation as a percentage of the sum of the intensities of the two cognate peptides. This method allowed to determine relative differences among light treatments of plants, regardless of the intrinsic physicochemical properties of the peptides which affect peptide flying in the quadrupole (Jin *et al.*, 2010; Konert *et al.*, 2015).

The phosphorylation stoichiometry for NALASALR was calculated summing the intensities (integrated peak area) of the four most intense transitions (Table S3 and Figure S2a,b) of the nonphosphorylated and phosphorylated form, respectively, according to the formula:

$$\%P = 100/[(t1+t2+t3+t4) + (pt1+pt2+pt3+pt4)] \times (pt1+pt2+pt3+pt4)$$

where %P is the percentage of phosphorylation, t1 t2… are the most intense transitions of the nonphosphorylated form and pt1 pt2… are the most intense transitions of the phosphorylated form.

For the phosphorylation stoichiometry of TVTETIDEISDGR, the intensities (integrated peak area) of the four most intense transitions of each peptide and phosphopeptide containing the sequence TVTETIDEISDGR, including the missed cleavage peptides (Table S3) were summed to generate the denominator of the formula described above, and the intensities of the four most intense transitions of the peptides bearing the phosphorylation on either Thr-537, Thr-541 or both were summed to give rise to the multiplying factor. No miss-cleavage peptides were ever found containing the sequence NALASALR, thus they were not used in the stoichiometry calculations.

To calculate the ratio between PsaB and PsaA as well as the ratios of these two proteins and STN7, respectively, the sum of the intensities of the three most intense transitions of the three most intense peptides (Table S3) were used.

The significance of the differences in percentage were calculated using a two-sided paired Student's *t*-test.

ACKNOWLEDGEMENTS

Research was financially supported by the Academy of Finland (project numbers 272424, 271832 and 273870), Doctoral Program in Molecular Life Sciences (DPMLS) as well as by Carl Tryggers Foundation. The Biocenter Finland and the Proteomics Facility of the Turku Centre for Biotechnology are thanked for the excellent support. Prof. Roberto Barbato and Drs Dorota Muth-Pawlak, Mikko Tikkanen, Sari Järvi and Petri Kouvonen are thanked for discussions, and Virpi Paakkarinen, Azfar Bajwa, Mika Keränen, Saara Mikola and Ville Käpylä for their excellent technical assistance.

CONFLICT OF INTEREST

The authors declare that they have no conflict of interest.

SUPPORTING INFORMATION

Additional Supporting Information may be found in the online version of this article.

Figure S1. Degradation kinetics of STN7 upon different light treatments of plants and the localization of the STN7 band in the SDS-PAGE gel by means of partial blotting.

Figure S2. Representative MS/MS spectrum and the corresponding SRM signal for different phosphopeptides of the STN7 kinase.

Figure S3. The sum of the intensities from the four most intense transitions of the phosphorylated and nonphosphorylated forms of NALASALR.

Figure S4. The single TVTETIDEISDGR phosphoforms in the WT and *tap38* plants and phosphorylations of STN7 in the *pbcp* plants.

Figure S5. SRM relative quantification of the STN7 protein from whole thylakoids of WT and *tap38* plants in comparison to the amount of the PSI core proteins PsaA and PsaB, and the amounts of the Lhcb1 and Lhcb2 proteins.

Table S1. Proteins identified in the band corresponding to STN7, sorted according to number of spectral counts (#PSM).

Table S2. List of peptides and phosphopeptides identified for STN7 in data-dependent analyses (DDA)

Table S3. List of transitions used to detect the peptides belonging to STN7, PsaA and PsaB in SRM. Highlighted in yellow are the transitions used to relatively quantify the phosphorylation levels and ratios between PsaA/PsaB and STN7.

REFERENCES

Alban, C., Tardif, M., Mininno, M. *et al.* (2014) Uncovering the protein lysine and arginine methylation network in Arabidopsis chloroplasts. *PLoS ONE*, **9**, e95512.

Aro, E.M. and Ohad, I. (2003) Redox regulation of thylakoid protein phosphorylation. *Antioxid. Redox Signal.* **5**, 55–67.

Bellafiore, S., Barneche, F., Peltier, G. and Rochaix, J.D. (2005) State transitions and light adaptation require chloroplast thylakoid protein kinase STN7. *Nature*, **433**, 892–895.

Brautigam, K., Dietzel, L., Kleine, T. *et al.* (2009) Dynamic plastid redox signals integrate gene expression and metabolism to induce distinct metabolic states in photosynthetic acclimation in *Arabidopsis*. *Plant Cell*, **21**, 2715–2732.

Buren, S., Ortega-Villasante, C., Blanco-Rivero, A., Martinez-Bernardini, A., Shutova, T., Shevela, D., Messinger, J., Bako, L., Villarejo, A. and Samuelsson, G. (2011) Importance of post-translational modifications for functionality of a chloroplast-localized carbonic anhydrase (CAH1) in *Arabidopsis thaliana*. *PLoS ONE*, **6**, e21021.

Depege, N., Bellafiore, S. and Rochaix, J.D. (2003) Role of chloroplast protein kinase Stt7 in LHCII phosphorylation and state transition in *Chlamydomonas*. *Science*, **299**, 1572–1575.

Grieco, M., Suorsa, M., Jajoo, A., Tikkanen, M. and Aro, E. M. (2015) Light-harvesting II antenna trimers connect energetically the entire photosynthetic machinery – including both photosystems II and I. *Biochim. Biophys. Acta*, **1847**, 607–619.

Jarvi, S., Suorsa, M., Paakkarinen, V. and Aro, E.M. (2011) Optimized native gel systems for separation of thylakoid protein complexes: novel super- and mega-complexes. *Biochem. J.* **439**, 207–214.

Jin, L.L., Tong, J., Prakash, A., Peterman, S.M., St-Germain, J.R., Taylor, P., Trudel, S. and Moran, M.F. (2010) Measurement of protein phosphorylation stoichiometry by selected reaction monitoring mass spectrometry. *J. Proteome Res.* **9**, 2752–2761.

Kauko, O., Laajala, T.D., Jumppanen, M., Hintsanen, P., Suni, V., Haapaniemi, P., Corthals, G., Aittokallio, T., Westermarck, J. and Imanishi, S.Y. (2015) Label-free quantitative phosphoproteomics with novel pairwise abundance normalization reveals synergistic RAS and CIP2A signaling. *Sci. Rep.* **5**, 13099.

Konert, G., Trotta, A., Kouvonen, P., Rahikainen, M., Durian, G., Blokhina, O., Fagerstedt, K., Muth, D., Corthals, G.L. and Kangasjarvi, S. (2015) Protein phosphatase 2A (PP2A) regulatory subunit B'gamma interacts with cytoplasmic ACONITASE 3 and modulates the abundance of AOX1A and AOX1D in *Arabidopsis thaliana*. *New Phytol.* **205**, 1250–1263.

Laemmli, U.K. (1970) Cleavage of structural proteins during the assembly of the head of bacteriophage T4. *Nature*, **227**, 680–685.

Lehtimaki, N., Koskela, M.M. and Mulo, P. (2015) Posttranslational modifications of chloroplast proteins: an emerging field. *Plant Physiol.* **168**, 768–775.

Lemeille, S., Willig, A., Depege-Fargeix, N., Delessert, C., Bassi, R. and Rochaix, J.D. (2009) Analysis of the chloroplast protein kinase Stt7 during state transitions. *PLoS Biol.* **7**, e45.

Lemeille, S., Turkina, M.V., Vener, A.V. and Rochaix, J.D. (2010) Stt7-dependent phosphorylation during state transitions in the green alga *Chlamydomonas reinhardtii*. *Mol. Cell Proteomics*, **9**, 1281–1295.

Liu, W., Tu, W., Liu, Y., Sun, R., Liu, C. and Yang, C. (2015) The N-terminal domain of Ihcb proteins is critical for recognition of the LHCII kinase. *Biochim. Biophys. Acta*, **1857**, 79–88.

Longoni, P., Douchi, D., Cariti, F., Fucile, G. and Goldschmidt-Clermont, M. (2015) Phosphorylation of the Lhcb2 isoform of light harvesting complex II is central to state transitions. *Plant Physiol.* **169**, 2874–2883.

MacLean, B., Tomazela, D.M., Shulman, N., Chambers, M., Finney, G.L., Frewen, B., Kern, R., Tabb, D.L., Liebler, D.C. and MacCoss, M.J. (2010) Skyline: an open source document editor for creating and analyzing targeted proteomics experiments. *Bioinformatics*, **26**, 966–968.

Martinsuo, P., Pursiheimo, S., Aro, E.M. and Rintamaki, E. (2003) Dithiol oxidant and disulfide reductant dynamically regulate the phosphorylation of light-harvesting complex II proteins in thylakoid membranes. *Plant Physiol.* **133**, 37–46.

Mazzoleni, M., Figureuet, S., Martin-Laffon, J., Mininno, M., Gilgen, A., Leroux, M., Brugiere, S., Tardif, M., Alban, C. and Ravanel, S. (2015) Dual targeting of the protein methyltransferase PrmA contributes to both chloroplastic and mitochondrial ribosomal protein L11 methylation in Arabidopsis. *Plant Cell Physiol.* **56**, 1697–1710.

Mekala, N.R., Suorsa, M., Rantala, M., Aro, E.M. and Tikkanen, M. (2015) Plants actively avoid state transitions upon changes in light intensity: role of light-harvesting complex II protein dephosphorylation in high light. *Plant Physiol.* **168**, 721–734.

Pesaresi, P., Hertle, A., Pribil, M. *et al.* (2009) Arabidopsis STN7 kinase provides a link between short- and long-term photosynthetic acclimation. *Plant Cell*, **21**, 2402–2423.

Piippo, M., Allahverdiyeva, Y., Paakkarinen, V., Suoranta, U.M., Battchikova, N. and Aro, E.M. (2006) Chloroplast-mediated regulation of nuclear genes in *Arabidopsis thaliana* in the absence of light stress. *Physiol. Genomics*, **25**, 142–152.

Porra, R.J., Thompson, W.A. and Kriedemann, P.E. (1989) Determination of accurate extinction coefficients and simultaneous-equations for assaying chlorophyll-a and chlorophyll-B extracted with 4 different solvents - verification of the concentration of chlorophyll standards by atomic-absorption spectroscopy. *Biochim. Biophys. Acta*, **975**, 384–394.

Pribil, M., Pesaresi, P., Hertle, A., Barbato, R. and Leister, D. (2010) Role of plastid protein phosphatase TAP38 in LHCII dephosphorylation and thylakoid electron flow. *PLoS Biol.* **8**, e1000288.

Rantala, M., Lehtimäki, N., Aro, E.-M. and Suorsa, M. (2016) Downregulation of TAP38/PPH1 enables LHCII hyperphosphorylation in Arabidopsis mutant lacking LHCII docking site in PSI. *FEBS L.* **590**, 787–794.

Reiland, S., Messerli, G., Baerenfaller, K., Gerrits, B., Endler, A., Grossmann, J., Gruissem, W. and Baginsky, S. (2009) Large-scale Arabidopsis phosphoproteome profiling reveals novel chloroplast kinase substrates and phosphorylation networks. *Plant Physiol.* **150**, 889–903.

Reiland, S., Finazzi, G., Endler, A. *et al.* (2011) Comparative phosphoproteome profiling reveals a function of the STN8 kinase in fine-tuning of cyclic electron flow (CEF). *Proc. Natl. Acad. Sci. U. S. A.* **108**, 12955–12960.

Rintamaki, E., Salonen, M., Suoranta, U.M., Carlberg, I., Andersson, B. and Aro, E.M. (1997) Phosphorylation of light-harvesting complex II and photosystem II core proteins shows different irradiance-dependent regulation in vivo. application of phosphothreonine antibodies to analysis of thylakoid phosphoproteins. *J. Biol. Chem.* **272**, 30476–30482.

Rintamaki, E., Martinsuo, P., Pursiheimo, S. and Aro, E.M. (2000) Cooperative regulation of light-harvesting complex II phosphorylation via the plastoquinol and ferredoxin-thioredoxin system in chloroplasts. *Proc. Natl. Acad. Sci. U. S. A.* **97**, 11644–11649.

Samol, I., Shapiguzov, A., Ingelsson, B., Fucile, G., Crevecoeur, M., Vener, A. V., Rochaix, J. D. and Goldschmidt-Clermont, M.(2012) Identification of a photosystem II phosphatase involved in light acclimation in Arabidopsis. *Plant Cell*, **24**, 2596–2609.

Schonberg, A. and Baginsky, S. (2012) Signal integration by chloroplast phosphorylation networks: an update. *Front. Plant. Sci.* **3**, 256.

Shapiguzov, A., Ingelsson, B., Samol, I., Andres, C., Kessler, F., Rochaix, J.D., Vener, A.V. and Goldschmidt-Clermont, M. (2010) The PPH1 phosphatase is specifically involved in LHCII dephosphorylation and state transitions in Arabidopsis. *Proc. Natl. Acad. Sci. U. S. A.* **107**, 4782–4787.

Suorsa, M., Rantala, M., Mamedov, F., Lespinasse, M., Trotta, A., Grieco, M., Vuorio, E., Tikkanen, M., Jarvi, S. and Aro, E.M. (2015) Light acclimation involves dynamic re-organization of the pigment-protein megacomplexes in non-appressed thylakoid domains. *Plant J.* **84**, 360–373.

Taus, T., Köcher, T., Pichler, P., Paschke, C., Schmidt, A., Henrich, C. and Mechtler, K. (2011) Universal and confident phosphorylation site localization using phosphoRS. *J. Proteome Res.* **10**, 5354–5362.

Vener, A.V., van Kan, P.J., Rich, P.R., Ohad, I. and Andersson, B. (1997) Plastoquinol at the quinol oxidation site of reduced cytochrome bf mediates signal transduction between light and protein phosphorylation: thylakoid protein kinase deactivation by a single-turnover flash. *Proc. Natl. Acad. Sci. U. S. A.* **94**, 1585–1590.

Wientjes, E., van Amerongen, H. and Croce, R. (2013) LHCII is an antenna of both photosystems after long-term acclimation. *Biochim. Biophys. Acta*, **1827**, 420–426.

Willig, A., Shapiguzov, A., Goldschmidt-Clermont, M. and Rochaix, J.D. (2011) The phosphorylation status of the chloroplast protein kinase STN7 of Arabidopsis affects its turnover. *Plant Physiol.* **157**, 2102–2107.

Wunder, T., Liu, Q., Aseeva, E., Bonardi, V., Leister, D. and Pribil, M. (2013) Control of STN7 transcript abundance and transient STN7 dimerisation are involved in the regulation of STN7 activity. *Planta*, **237**, 541–558.